

Temperature measurements in gases using laser-induced electrostrictive gratings

A. Stampanoni-Panariello, B. Hemmerling, W. Hubschmid

Paul Scherrer Institut, CH-5232 Villigen PSI, Switzerland
 (Fax: +41-56/310-2199, E-mail: Anna.Stampanoni@psi.ch)

Received: 1 December 1997 / Revised version: 27 January 1998

Abstract. We used time-resolved light scattering from electrostrictive gratings for the determination of temperatures in gases at atmospheric pressure. The infrared radiation from a pulsed Nd:YAG laser generates the grating and the beam of a cw laser reads it out. We evaluated this technique by measurements in a tube furnace for temperatures up to 1370 K. Furthermore, temperature determinations are carried out in premixed methane/air and carbon monoxide/oxygen flames.

PACS: 42.62.b; 42.65.Es; 78.20.Hp

The constraints on pollutant production by fossil combustion processes have increased during recent years promoting the development of sophisticated combustion technologies. To speed up this evolution process there is a demand to employ advanced computational design tools which in turn have to be validated by non-invasive diagnostic methods. Among optical diagnostic techniques coherent anti-Stokes Raman scattering, CARS, is the most established and accepted method for the non-intrusive determination of gas temperature in combustion processes [1]. However, especially at high pressure, this technique suffers from an inherent complexity which inhibits on-line temperature measurements [2]. Recently, laser-induced gratings have been proposed as an alternative [3]. They carry the promise of being a simple method to determine temperatures in particular at elevated pressures.

Laser-induced gratings arise from the interference of two excitation beams intersecting in a medium. The interference produces a spatially periodic light intensity distribution which may change the complex refractive index of the medium by various resonant or non-resonant mechanisms [4]. Electrostrictive gratings are generated at any frequency of the excitation beams [5]. The electric field of the interference structure polarizes the dielectric medium and the spatial inhomogeneity of the field causes a motion of mass towards regions of high laser intensity. Sound waves are generated, with the wavelength being defined by the fringe spacing of the interference pattern. They propagate in two opposite directions, normal to the planes of the fringes. The counter-propagating sound waves form a standing acoustic wave and

thereby a spatially periodic density grating that oscillates in time. Satisfying the Bragg condition this grating can be read out by the beam of another laser.

The sensitivity of resonant, laser-induced grating spectroscopy may be limited by the occurrence of an electrostrictive grating contribution [6]. On the other hand, laser-induced electrostrictive gratings, LIEGs, are already proposed for diagnostic purposes. This has been illustrated by imaging a stream of helium in air [7]. Cummings [8] and Stampanoni et al. [9] showed the possibility of using LIEGs to measure sound velocity and acoustic attenuation in gases.

We report on, to our knowledge, the first application of LIEGs for the determination of temperatures in gases at atmospheric pressure. The technique has been evaluated by measurements in a tube furnace up to a maximum temperature of about 1370 K. Furthermore, two examples of temperature determinations in flames are given.

1 Theoretical considerations

The reflectivity of a laser-induced grating is, see for example [4],

$$R = \frac{I_S}{I_R} \left(\frac{\pi \Delta n d}{\lambda_R} \right)^2 + \left(\frac{\Delta K d}{4} \right)^2 \quad (1)$$

where I_R and I_S are the intensities of the read-out and scattered beams, d is the thickness of the grating, λ_R is the wavelength of the read-out laser, and Δn and ΔK are the changes in the refractive index and in the absorption coefficient across a fringe of the grating, respectively. If there is no absorption at the wavelength of the laser reading out the grating, a pure phase grating is obtained. In a gas the thermo-optic coefficient ($\partial n / \partial T$) is usually small and can be neglected in comparison to the change in the refractive index caused by a variation of the density. The density change effected by electrostriction and by the release of resonantly absorbed laser energy in the form of heat can be quantitatively described by the linearized hydrodynamic equations [10]. The solution of this system of coupled equations is a stationary (non-oscillating) density

modulation superimposed on a standing acoustic wave [11, 12]. The approximate expression for the oscillation frequency of the density is [13]

$$\Omega = qv \left[1 + \left(\frac{T_p}{\pi\tau} \right)^2 \right]^{-1/2} \quad (2)$$

where T_p is the oscillation period of the density, v is the adiabatic sound velocity, and q is the grating vector,

$$q = \frac{2\pi}{\Lambda} . \quad (3)$$

Here, Λ is the fringe spacing of the grating generated by the two excitation beams of wavelength λ_E , intersecting at an angle θ ,

$$\Lambda = \frac{\lambda_E}{2 \sin(\theta/2)} . \quad (4)$$

The density variation decays with the time constant [9]

$$\tau = \left(\frac{q^2}{2\rho_0} \left[\eta + \frac{(\gamma-1)\kappa}{c_p} \right] \right)^{-1} , \quad (5)$$

where $\eta = (4/3)\eta_s + \eta_b$ is the viscosity, η_s is the shear viscosity and η_b is the bulk viscosity, κ is the thermal conductivity, $\gamma = c_p/c_v$ the ratio of the specific heat capacities, and ρ_0 the equilibrium density of the medium.

If no absorbed laser energy is released in the form of heat, the amplitude of the stationary density modulation is much smaller than that of the standing acoustic wave. In this case, which applies for pure electrostriction, the density oscillates around its undisturbed value leading to an oscillation of the grating reflectivity with a frequency of 2Ω . If the main contribution to the density variation is caused by fast heat release the stationary density modulation and the standing acoustic wave have the same amplitude [12]. The density oscillates in this case around a value given by the stationary grating contribution, and the grating reflectivity has an oscillation frequency Ω .

With the help of (2) one can determine the sound velocity of the medium from the time-resolved measurement of the grating reflectivity. For an ideal gas the sound velocity is related to the temperature by

$$v = \sqrt{\frac{TR\gamma}{M}} \quad (6)$$

where M is the effective molar mass of the gas mixture, and R the universal gas constant.

2 Experimental

A scheme of the experimental setup is depicted in Fig. 1a. The two grating excitation beams, with a wavelength of 1064 nm, are provided by a pulsed Nd:YAG laser (Continuum, NY81-20). The pulse length of the laser is about 8 ns, and the

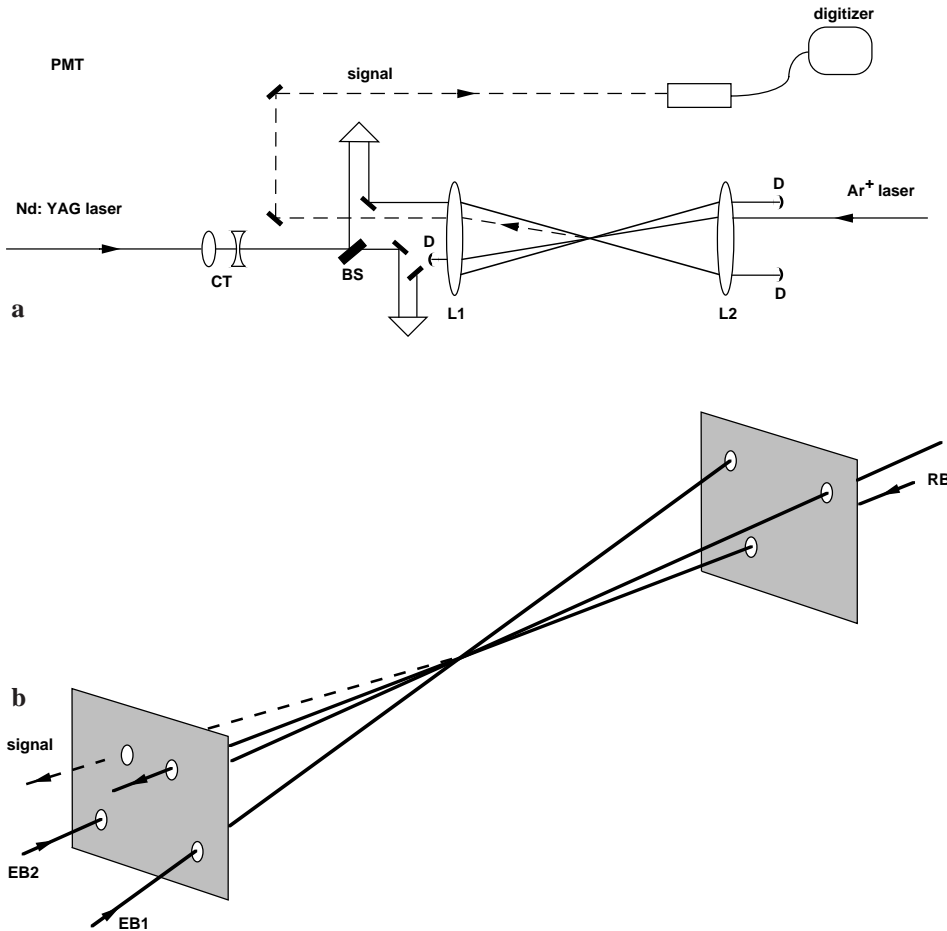


Fig. 1. **a** Experimental setup (CT, cylinder telescope ($f_1 = +300$ mm, $f_2 = -100$ mm); BS, beam splitter ($R = 50\%$); L1, L2, lenses ($f = 750$ mm); D, beam dump; PMT, photomultiplier (Philips XP2020)). **b** 3D backward phase matching geometry (EB1, EB2, grating excitation beams ($\lambda_E = 1064$ nm); RB, read-out beam ($\lambda_R = 514$ nm))

spectral bandwidth of the radiation has a FWHM of 1 cm^{-1} . Without amplifier, the output energy of the laser is about 140 mJ/pulse and with amplifier about 320 mJ/pulse. The laser-induced grating is read out by the beam of a cw Ar⁺ laser (Spectra Physics 587 Z-LOK), operated at a single line at 514.5 nm with a power of approximately 1.7 W. We used a 3D backward geometry to obtain phase matching of the three beams (see Fig. 1b). The signal leaves the interaction volume counter-propagating to the direction of the excitation beams. It is collimated and directed over a path of 5 m onto the aperture of a photomultiplier tube (Philips XP2020). The time-resolved acquisition of the signal is performed by a digitizer (Tektronix, RTD 720) with a full bandwidth of 500 MHz and a 2-GHz sampling rate.

Using the fundamental wavelength of the Nd:YAG laser for grating generation is convenient for the following reasons. Since the photomultiplier is not sensitive to infrared radiation, stray light caused by the excitation beams is suppressed without the use of any frequency filter in the signal beam path. For most of the gases the threshold for optical breakdown is higher at longer wavelengths [14] allowing higher excitation energies per pulse to be employed. The scattering efficiency of the grating increases with a decreasing ratio λ_R/λ_E because the probe beam must cross the grating region at a smaller angle in order to satisfy the Bragg condition, thus increasing the effective path length through the grating region. Finally, for a given crossing angle of the excitation beams, the grating spacing is larger for a longer excitation wavelength resulting in a larger time constant for the decay of the density modulation (see (5)).

The obtainable spatial resolution of the LIEG technique is determined by the size of the interaction volume of the excitation beams and the read-out beam [15]. Focusing of the beams reduces the size of the interaction volume, but increases the effect of sound propagation out of this small volume considerably. This results in a shorter lifetime of the standing acoustic wave, i.e., in a decrease in the number of observable oscillations of the grating reflectivity. To reduce this effect, the cross section of the excitation beam is formed into a stripe (6 mm high and 1 mm wide, approximately) by means of a telescope consisting of two cylindrical lenses. Subsequently, this beam passes a 50% beam splitter. The two resulting excitation beams are directed through separate delay lines to achieve equal optical path lengths for both beams. The parallel propagating excitation beams are crossed at an angle $\theta = 1.5^\circ$ by focusing them through the same lens ($f = 750 \text{ mm}$). Due to diffraction, the heights of the excitation beams are focused tighter than their widths resulting in a strip-shaped focus approximately 1 mm wide and 250 μm high. The orientation of the strip-shaped excitation beams with respect to their plane of incidence is chosen so that the direction of the larger extension of the grating volume coincides with the propagation direction of the sound waves.

3 Results and discussion

We determined the spatial resolution experimentally by translating a helium flow across the grating volume along the direction of the bisector of the two excitation beams. The helium emerged in ambient air from the circular outlet (diameter 5 cm) of a flat-flame burner, described later on in this

article. Compared to air, the grating reflectivity in helium is smaller by a factor of about 64. In Fig. 2 the total grating signal is plotted versus the relative shift between helium flow and grating volume. The zero point of the movement was selected arbitrarily in such a way that the grating volume was entirely within the helium flow. The solid line depicted in Fig. 2 is a fit to the data points by a cumulative normal distribution (error function) resulting in a standard deviation of the normal distribution of $\sigma = 4.1 \pm 0.7 \text{ mm}$. Therefore, about 95% of the signal is generated in a volume extending $4\sigma = 16.4 \pm 2.8 \text{ mm}$ in the direction of the bisector of the two excitation beams. Certainly, there is no sharp boundary of the helium flow in air. No attempt was undertaken to account for edge effects and their influence on the determined spatial resolution.

To evaluate the error in temperatures measured by LIEGs, we performed measurements in an open tube furnace up to a maximum temperature of 1370 K. The length of the isothermal zone ($\sigma = 5 \text{ K}$) within the furnace exceeds 10 cm at all temperatures. The temperature reading of the furnace was taken by means of a thermocouple located in the center of the heated zone. We carried out LIEG measurements in air at different furnace temperatures. At temperatures above 600 K measurements were performed with and without amplifier of the Nd:YAG laser. Besides a better signal-to-noise ratio at higher output powers of the Nd:YAG laser we observed no systematic discrepancy for the determined oscillation periods.

At 1370 K the decay time of the grating reflectivity is more than twice as long as the oscillation period of the density. Therefore, for temperatures up to 1370 K the term in brackets in (2) can be safely approximated by 1.0 and one gets for the sound velocity

$$v = \frac{\Lambda}{T_p}. \quad (7)$$

To avoid the determination of the fringe spacing Λ by a geometric measurement of the crossing angle θ we carried out a reference measurement at room temperature in ambient air.

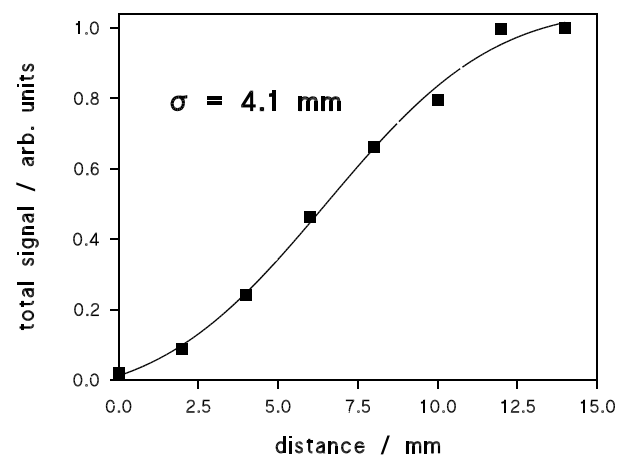


Fig. 2. Determination of the spatial resolution of the LIEG technique. The total LIEG signal is plotted vs the relative shift between helium flow and grating volume (see text). The data are fitted by an error function (solid line)

By using (6), the measured temperature is given by

$$T = T_R \left(\frac{T_{P,R}}{T_{P,T}} \right)^2 \left(\frac{\gamma_R}{\gamma_T} \right) \left(\frac{M_T}{M_R} \right). \quad (8)$$

Here, the subscripts R and T refer to reference and temperature measurement, respectively. Because of the large number of visible peaks in the temporal evolution of the LIEG signal at room temperature the relative standard deviation in the oscillation period $T_{P,R}$ is 0.77%. For the measurements in air we assumed that the ratio of the relative molecular masses is unity.

In Fig. 3 the LIEG temperatures are plotted versus the temperature reading of the furnace. For clarity, a broken line that corresponds to equality of the two temperatures is also shown. With increasing temperature a decreased gas density, together with increased values of heat conduction and viscosity, leads to a reduction in signal strength and to a smaller number of visible peaks in the temporal evolution of the LIEG signal. This results in an increased standard deviation for the oscillation period and thereby in an increased error for the temperature measurement. Although the LIEG temperature agrees with the temperature reading of the furnace within the error bars, there is some evidence that the LIEG temperature is systematically too high. To determine the temperature from the measured oscillation period of the LIEG signal, one has to rely on tabulated values of sound velocity or specific heat ratio as a function of temperature [16, 17]. Normally, changes in the gas composition caused by thermo-diffusion or dissociation are not accounted for in these tables. Furthermore, due to the high frequency of the generated sound waves ($\nu \approx 8$ MHz), one also has to be aware of dispersion and its temperature dependence [18]. However, tabulated values of the sound velocity will, in such cases, be a lower limit to the actual velocity which in turn would lead to lower LIEG temperatures. Certainly, a more quantitative discussion of the influences of all these effects on the sound velocity is necessary if a systematic deviation of the LIEG temperature is proved by more precise measurements. These can be expected for LIEG temperature determinations in high-pressure environments.

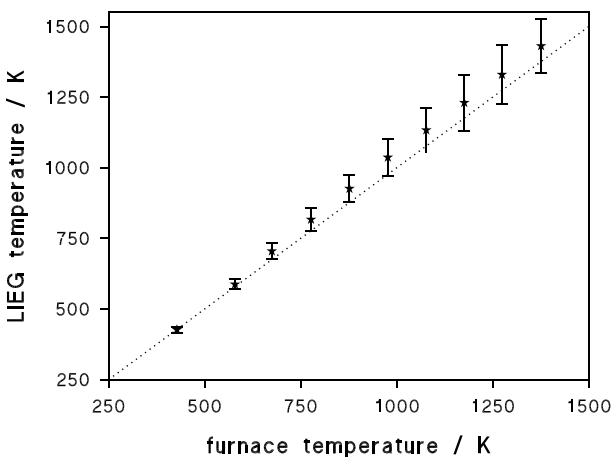


Fig. 3. Temperature measurement in air at atmospheric pressure by LIEG vs temperature measurement by a thermocouple inside the furnace. The signal was averaged over 100 shots. The *dotted line* corresponds to an equality of the two temperature measurements

To assess the statistical error of single-shot temperature determination by the LIEG technique, a number of single-shot measurements have been carried out at a furnace temperature of 1370 K. We considered 100 single-shot spectra to be a good basis for a statistical analysis. The temperatures were compiled in a normalized histogram with a temperature interval of 10 K. Together with the histogram of the measured temperatures Fig. 4 displays a Gaussian probability function (dotted line) with mean temperature and standard deviation fitted to the data. From the measurements one can deduce a mean temperature of 1470 K, with a standard deviation of 72 K. The width of the distribution essentially reflects the principal uncertainty of the measurement. The consistency with the Gaussian distribution implies that random processes are responsible for the observed temperature fluctuations. Because of the limited photon flux these fluctuations may arise from the photoelectron statistics and the quantization noise of the digitizer.

We used LIEGs for temperature determinations in laminar, premixed flames at atmospheric pressure. The measurements were performed by means of a flat-flame burner with a 5-cm-diameter, water-cooled, sintered stainless steel flame holder surrounded by a guard ring for isolating the flame from the ambient air. Mass flow controllers, assuring stable operating conditions, were employed to adjust the equivalence ratio. The measurement volume was located about 2 mm above the burner surface and the Nd:YAG laser was operated without amplifier. Although the signal intensity was averaged over 100 shots, its temporal signature still exhibits distortion because of the limited photon flux. Figure 5 shows the temporal signature of the grating reflectivity, which was obtained in a stoichiometric methane/air flame. One can determine an oscillation period of 43.3 ns, with a standard deviation of 2.5 ns. However, the temporal evolution of the signal begins with a small peak which does not fit into this period and which cannot be attributed to scattered light from the Nd:YAG laser. With the gas composition known from equilibrium calculations, and the measured oscillation period, one calculates for the flame temperature a value of 580 K. For a stoichiometric methane/air flame at atmospheric pressure a temperature of

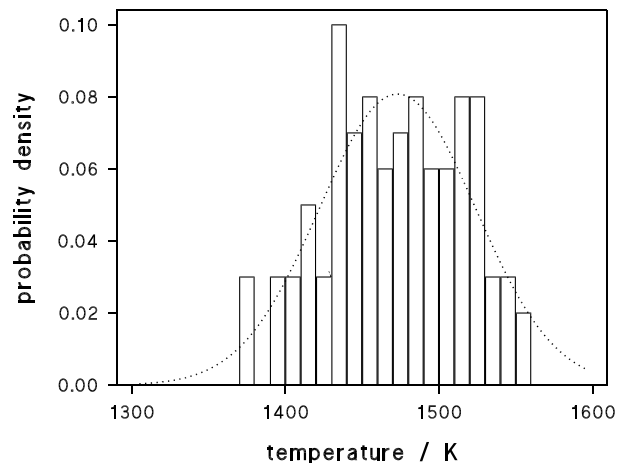


Fig. 4. Single-shot LIEG temperature measurements in air at a furnace temperature of 1376 K. The temperatures are compiled in a normalized histogram with a temperature interval of 10 K. The *dotted line* corresponds to a Gaussian probability function with mean temperature and standard deviation fitted to the data

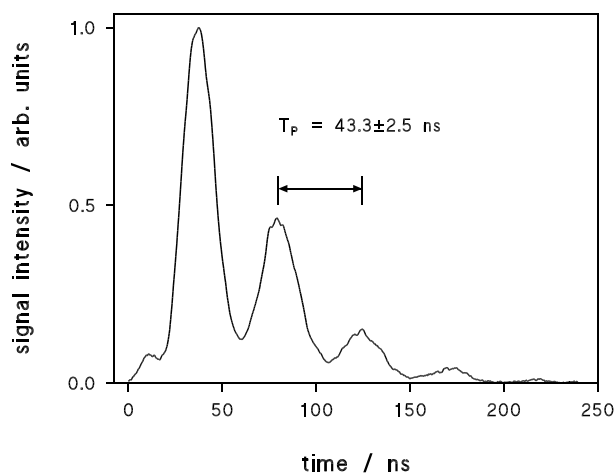


Fig. 5. Measurement in a stoichiometric CH₄/air flame performed at a height of about 2 mm above the burner surface. The signal is averaged over 100 shots. From the measured oscillation period of the signal a temperature of 2342 ± 245 K is determined

2065 ± 50 K is an established value [19]. Led by this strong discrepancy in the measured temperature, and by the appearance of the small peak at the beginning of the temporal evolution of the LIEG signal, we made the assumption that there is absorption at the wavelength of the excitation laser. Therefore, the observed signal would be mainly caused by a thermal grating exhibiting an oscillation period twice as long as that of an electrostrictive grating. With this assumption we determined the flame temperature as 2342 ± 245 K.

Measurements in a stoichiometric hydrogen/air flame also showed an oscillation period about twice as long as expected. Therefore, the most probable candidates for causing absorption at the fundamental wavelength of the Nd:YAG laser turned out to be H₂O and OH. A search in the HITEMP [20] database, containing a file with transitions in water vapor at 1500 K, delivered four absorption lines of H₂O within the spectral bandwidth of the Nd:YAG laser.

To establish the assumption of generating a thermal grating by H₂O hot-band absorption lines, we carried out additional measurements in a premixed, laminar carbon monoxide/oxygen flame. In this case the Nd:YAG laser was operated with amplifier. However, the signal level is very low and is dominated by single-photon events. Figure 6 shows the temporal development of the LIEG signal averaged over 100 shots in a stoichiometric flame. The measurement location was 2 mm above the burner surface. We determined an oscillation period of the grating reflectivity of 23.7 ns with a standard deviation of 1.3 ns. The local gas composition in the measurement volume was determined by calculating a one-dimensional, freely propagating flame. The mole fractions of the major species are $X_{\text{CO}_2} = 0.39$, $X_{\text{CO}} = 0.37$, and $X_{\text{O}_2} = 0.15$. From the oscillation period and the gas composition we calculated a temperature of 2630 ± 240 K. This value agrees fairly well with the value of 2460 K from the model calculation. However, conduction of heat to the burner plate, which lowers the adiabatic flame temperature, was not taken into account. The fairly good agreement between the measured and calculated temperatures allows us to conclude that the observed signal is caused solely by electrostriction.

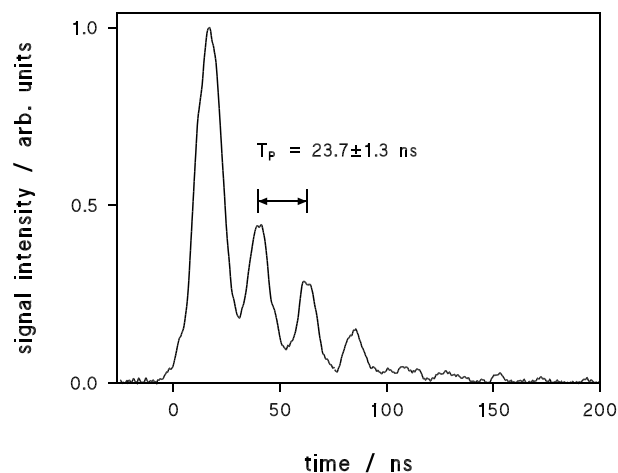


Fig. 6. LIEG signal vs time obtained in a stoichiometric CO/O₂ flame at a height of 2 mm above the burner surface. The signal is averaged over 100 shots. From the measured oscillation period and the gas composition a temperature of 2630 ± 240 K is determined

4 Conclusions

Laser-induced electrostrictive gratings have been used for temperature determinations at atmospheric pressure in air and in flames. To evaluate the error in this technique we performed measurements in an open tube furnace up to a maximum temperature of 1370 K. Although temperatures measured by the LIEG method agree within the error bars with the thermocouple readings there is some evidence that the LIEG temperatures are systematically too high. For single-shot temperature measurements in air we determine a statistical error of 72 K at a furnace temperature of 1370 K.

LIEG measurements in a premixed, stoichiometric methane/air flame revealed a strong thermal grating contribution to the signal caused by H₂O hot-band absorption. As expected this contribution is absent in a carbon monoxide/oxygen flame. The signal-to-noise ratio obtained in both flames is poor due to low gas density and strong attenuation of the grating by heat conduction and viscosity. Better signal-to-noise ratios are expected for flames at high pressure. The application of this technique to high-pressure environments is under investigation and will be published in a forthcoming paper.

Acknowledgements. We are indebted to Dr. I. Mantzaras for performing the calculation of a one-dimensional freely propagating CO/O₂ flame. This work is financially supported by the Swiss Federal Office of Energy (BEW).

References

1. A.C. Eckbreth: *Laser Diagnostics for Combustion Temperature and Species* (Abacus, Cambridge, MA 1988)
2. M. Woyde: PhD Thesis, University of Stuttgart, Germany 1992
3. S. Williams, L.A. Rahn, P.H. Paul, J.W. Forsman, R.N. Zare: *Opt. Lett.* **19**, 1681 (1994)
4. H.J. Eichler, P. Günter, D.W. Pohl: *Laser-Induced Dynamic Gratings*, Springer Ser. Opt. Sci., Vol. 50 (Springer, Berlin, Heidelberg 1986)
5. K.A. Nelson, D.R. Lutz, M.D. Fayer, L. Madison: *Phys. Rev. B* **24**, 3261 (1981)
6. D.E. Govoni, J.A. Booze, A. Sinha, F.F. Crim: *Chem. Phys. Lett.* **216**, 525 (1993)
7. B. Hemmerling, A. Stampanoni-Panariello: *Appl. Phys. B* **57**, 281 (1993)
8. E.P. Cummings: *Opt. Lett.* **19**, 1361 (1994)

9. A. Stampanoni-Panariello, B. Hemmerling, W. Hubschmid: Phys. Rev. A **51**, 655 (1995)
10. R.W. Boyd: *Nonlinear Optics* (Academic Press, New York 1992) p. 325
11. P.H. Paul, R.L. Farrow, P.M. Danehy: J. Opt. Soc. Am. B **12**, 384 (1995)
12. W. Hubschmid, B. Hemmerling, A. Stampanoni-Panariello: J. Opt. Soc. Am. B **12**, 1850 (1995)
13. W. Hubschmid, R. Bombach, B. Hemmerling, A. Stampanoni-Panariello: Appl. Phys. B **62**, 103 (1996)
14. G.M. Weyl: In *Laser-Induced Plasmas and Applications*, ed. by L.J. Radziemski, D.A. Cremers (Marcel Dekker Inc. 1989) p. 1
15. A.E. Siegman: J. Opt. Soc. Am. **67**, 545 (1977)
16. J.H. Keenan, J. Chao, J. Kaye: *Gas Tables*, 2nd edn. (Wiley, New York 1980)
17. J. Hilsenrath, C.W. Beckett, W.S. Benedict, L. Fano, H.J. Hoge, J.F. Masi, R.L. Nuttall, Y.S. Touloukian, H.W. Woolley: *Tables of Thermal Properties of Gases* (National Bureau of Standards, Washington, D.C. 1955)
18. H.O. Kneser: *Schallabsorption und -dispersion in Gasen*, Handbuch der Physik, Bd. XI/1
19. A. Lawitzki, I. Plath, W. Stricker, J. Bittner, U. Meier, K. Kohse-Höinghaus: Appl. Phys. B **50**, 513 (1990)
20. L.S. Rothman, R.B. Wattson, R.R. Gamache, D. Goorvitch, R.L. Hawkins, J.E.A. Selby, C. Camy-Peyret, J.-M. Flaud, J. Schroeder, A. McCann: to be published in J. Quant. Spectrosc. Radiat. Transfer